Attitude control laws validation through probabilistic μ-analysis: application to microsatellite control laws

Hélène Evain, Tommaso Casati, Clément Roos, Jean-Marc Biannic

ATTITUDE CONTROL LAWS VALIDATION THROUGH PROBABILISTIC μ-ANALYSIS: APPLICATION TO MICROSATELLITE CONTROL LAWS

Hélène Evain [1], Tommaso Casati [1,2], Clément Roos [3], Jean-Marc Biannic [3]

[1] CNES, 18 Avenue Edouard Belin, 31400 Toulouse, +33561274070, helene.evain@cnes.fr
[1] CNES, 18 Avenue Edouard Belin, 31400 Toulouse, tommaso.casati@cnes.fr
[2] Politecnico di Milano, Department of Aerospace Engineering, 20133 Milano
[3] ONERA, 2 Avenue Edouard Belin, 31400 Toulouse, clement.roos@onera.fr
[3] ONERA, 2 Avenue Edouard Belin, 31400 Toulouse, jean-marc.biannic@onera.fr

ABSTRACT

With the growing complexity of space missions, the validation & verification (V&V) phase in AOCS design becomes very time-consuming. Based on a realistic microsatellite design example, the objective of this paper is to show how recent advances in the development of μ-analysis and probabilistic μ-analysis tools can be used to improve the efficiency of controllers' robustness analysis before the Monte-Carlo simulation campaigns. More precisely, after a brief presentation of the tools, it is shown how they can be integrated in a current V&V process and what can be expected next.

1 INTRODUCTION

During the development of a new attitude control system for ambitious satellite missions, the validation & verification (V&V) phase represents a large part of the process, up to 80% of the time spent for AOCS design. One difficulty is to detect worst-case configurations of parameters to ensure robustness of the designed controllers. When applicable, μ-analysis [1, 2] offers a nice additional tool to be used before launching the Monte Carlo simulation campaign, but it does not provide any quantification of the probability of occurrence of the identified worst-cases. A control system can then be invalidated on the basis of unlikely events. Probabilistic μ-analysis [3, 4] was introduced in this context more than 20 years ago to bridge the gap between the two techniques, with the ambition to quantify the probability of (very) rare but potentially critical events. It has been used for the first time in [5] in the challenging context of launcher thrust vector control systems validation. But it appeared to be computationally very expensive. At that time indeed, no practical tool offering both good reliability and reasonable computational time was available, making this technique hardly usable in an industrial context. More recently, following the work carried out in [6, 7], significant improvements have been achieved by ONERA supported by ESA and CNES to develop the STOchastic Worst-case Analysis Toolbox (STOWAT) [8, 9, 10]. With the help of this new Matlab toolbox, probabilistic μ-analysis may now be considered as a very good candidate for integration in the aerospace V&V process in a near future, finding its place between Monte Carlo simulations – useful for quantifying the probability of sufficiently frequent phenomena – and worst-case μ-analysis – relevant for detecting extremely rare events. Recently tested on a series of AOCS benchmarks of increasing complexity [9], the most recent version of the toolbox is now evaluated on a challenging and realistic attitude control problem that was faced in a microsatellite project at CNES.

The first part of this paper describes the probabilistic μ-analysis framework and the latest improvements made to the STOWAT. Then, a description of the Microcarb satellite application case is provided, with an emphasis on the normal mode (MNO) and the orbit control mode (MCO) in the AOCS architecture. Finally, the preliminary validation process, before Monte-Carlo simulations are performed, is compared when using either (probabilistic) μ-analysis or more classical tools, and a critical assessment is provided.

2 RECENT ADVANCES IN PROBABILISTIC μ-ANALYSIS

Let us consider the following continuous-time uncertain Linear Time-Invariant (LTI) system:

$$\begin{cases} \dot{x} = A(\delta)x + B(\delta)u \\ y = C(\delta)x + D(\delta)u \end{cases} \tag{1}$$

where $x \in \mathbb{R}^n$, $u \in \mathbb{R}$ and $y \in \mathbb{R}$ represent the system states, scalar input and scalar output respectively. The real uncertain parameters $\delta = (\delta_1, \dots, \delta_N) \in \mathbb{R}^N$ are bounded and belong to the uncertainty domain $\mathcal{D}_\delta = \left[\underline{\delta}_1 \ \overline{\delta}_1\right] \times \dots \times \left[\underline{\delta}_N \ \overline{\delta}_N\right]$. It is assumed without loss of generality that they are normalized (which can always be done using an affine transformation), *i.e.* $\mathcal{D}_\delta = \mathcal{B}_\delta = [-1 \ 1]^N$. Moreover, they are independent random variables, whose probability density functions f are supported on the bounded interval $[-1 \ 1]$. Uniform and truncated normal distributions are often used in practice, but any other distribution supported on a bounded interval can be used.

It is assumed that $A(\delta), B(\delta), C(\delta), D(\delta)$ are polynomial or rational functions of the δ_i and that system (1) can be transformed into a Linear Fractional Representation (LFR) as in Figure 1: the uncertainties are separated from the nominal LTI system $M(s)$ and isolated in a block-diagonal operator $\Delta = diag\left(\delta_1 I_{n_1}, \dots, \delta_N I_{n_N}\right)$, where I_{n_i} is the $n_i \times n_i$ identity matrix. The question of how this transformation is performed and in which cases exactly it is possible is out of the scope of this paper, but more information can be found in [1]. The set of matrices with the same block-diagonal structure as Δ is denoted $\mathbf{\Delta}$. Let then $\mathcal{B}_{\mathbf{\Delta}} = \{\Delta \in \mathbf{\Delta} : \delta_i \in \mathcal{B}_\delta\}$ be the subset of $\mathbf{\Delta}$ corresponding to $\mathcal{B}_\delta$.

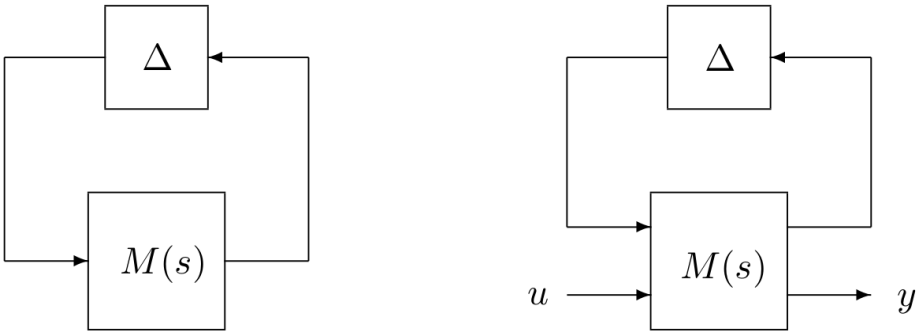

Figure 1. Standard interconnections for robust stability (left) and performance or gain/phase/disk/delay margin (right) analysis

With these notations in mind, three main problems can currently be solved using probabilistic μ-analysis. Stability analysis is introduced first and the corresponding interconnection is shown in Figure 1 (left). It is assumed that system (1) – and therefore $M(s)$ – represents the closed-loop interconnection between a physical plant and a control law (*e.g.* a satellite with its AOCS).

Problem 1 (Probabilistic robust stability). Compute the probability $\overline{P}_{\mathbf{\Delta},f}\big(M(s)\big)$ that the interconnection of Figure 1 (left) is unstable when $\Delta \in \mathcal{B}_{\mathbf{\Delta}}$.

H_∞ performance analysis is considered next and the corresponding closed-loop interconnection is shown in Figure 1 (right). Let $\mathcal{T}_{u\to y}(s,\Delta)$ denote the closed-loop transfer from u to y.

Problem 2 (Probabilistic robust H_∞ performance). Given a performance level $\gamma > 0$, compute the probability $\overline{P}^{\gamma}_{\mathbf{\Delta},f}\big(M(s)\big)$ that $\left\|\mathcal{T}_{u\to y}(s,\Delta)\right\|_\infty > \gamma$ on Figure 1 (right) when $\Delta \in \mathcal{B}_{\mathbf{\Delta}}$.

In the perspective of computing robust stability (*i.e.* gain, phase, disk and delay) margins, system (1) – and therefore $M(s)$ – now describes the considered control loop, opened at the place where the margins have to be computed. In other words, the closed-loop interconnection is recovered by applying a unit negative feedback between y and u in Figure 1 (right). With this in mind, probabilistic stability margins analysis can be formalized as follows:

Problem 3 (Probabilistic robust stability margins). Compute the probability $\overline{P}^{\phi}_{\mathbf{\Delta},f}\big(M(s)\big)$ that the gain, phase, disk or delay margin is less than a given threshold ϕ when $\Delta \in \mathcal{B}_{\mathbf{\Delta}}$ for the negative feedback loop obtained by connecting y to u in Figure 1 (right).

Once computed, each of these probabilities can be confronted to a given tolerance level $\mathcal{E}$, so as to validate or reject the considered control system, depending on whether it is lower or higher than $\mathcal{E}$.

During the past 5 years, a significant effort has been put in the development of probabilistic μ theory and its implementation in the Matlab STOchastic Worst-case Analysis Toolbox (STOWAT) [9]. Stability and H_∞ performance were studied first [7, 8], followed by gain/phase/disk margins [10] and more recently delay margin [11]. The theory behind μ-analysis is not presented in this paper due to space limitations, but the interested reader can for example refer to [1, 2, 12] and [3–11] for the classical and the probabilistic versions respectively. Only a few facts are briefly recalled below to facilitate the understanding of the paper.

Classical μ-analysis is based on the computation of the structured singular value $\mu_{\mathbf{\Delta}}$ on the whole frequency range. This computation being NP-hard in general, upper and lower bounds are usually determined instead of the exact value. Much work has been done in the past decades to reduce the gap between these bounds, and (almost) exact values are now obtained in most cases with a reasonable computational time [13]. The main reason why the gap sometimes remains non-negligible and the computational time significant is the presence of uncertainties repeated many times in Δ, *i.e.* high values of some n_i.

Probabilistic μ-analysis combines the aforementioned μ-based tools with a Branch-and-Bound (B&B) algorithm to explore the whole uncertainty domain $\mathcal{B}_\delta$. A simple stability test is first performed at the center of the domain, *i.e.* for $\Delta = 0$. If the resulting system is stable (resp. unstable), stability (resp. instability) is then investigated on $\mathcal{B}_\delta$ using sufficient conditions involving μ upper bound computations. If it cannot be guaranteed on the entire domain, $\mathcal{B}_\delta$ is finally partitioned into smaller boxes and this process is repeated until each box has guaranteed stability/instability or is sufficiently small to be neglected (see Algorithm 1 of [7]). This leads to the following partition of the uncertainty domain:

$$\mathcal{B}_\delta = D_s \cup D_{\overline{s}} \cup D_{s_u}$$

where D_s, $D_{\overline{s}}$ and D_{s_u} are three sets of disjoint N-cubes corresponding to the domains where stability is guaranteed, instability is guaranteed and stability is undetermined respectively, with probabilities $p(D_s)$, $p(D_{\overline{s}})$ and $p\left(D_{s_u}\right)$. The domain D_{s_u} stems from the aforementioned NP-hardness issue, but also from the fact that B&B can only approximate D_s and $D_{\overline{s}}$, and not compute them exactly. The probability $p\left(D_{s_u}\right)$ can be reduced by increasing the number of iterations of the algorithm, at the price of an increase in the CPU time. Guaranteed lower and upper bounds on the exact probability $\overline{P}_{\mathbf{\Delta},f}\left(M(s)\right)$ of instability are finally obtained as follows, thus solving Problem 1:

$$p(D_{\overline{s}}) \leq \overline{P}_{\mathbf{\Delta},f}\left(M(s)\right) \leq 1 - p(D_s) = p(D_{\overline{s}}) + p\left(D_{s_u}\right)$$

Their accuracy depends on the chosen stopping criterion of the B&B algorithm, which allows to handle the trade-off between accuracy and computational time.

Performance analysis can be done in the same way. On the one hand, a μ-based sufficient condition to guarantee H_∞ performance on a box – $\left\|\mathcal{T}_{u\to y}(s,\Delta)\right\|_\infty \leq \gamma$ – is easily obtained using the main loop theorem [14]. On the other hand, checking whether non-performance is guaranteed – $\left\|\mathcal{T}_{u\to y}(s,\Delta)\right\|_\infty > \gamma$ – requires to solve a minimax problem, which cannot be directly reformulated in the μ framework. Nevertheless, a sufficient condition is proposed in [7] (see Proposition 3.1 and Algorithm 2) to overcome this issue. This leads to the following partition of D_s:

$$D_s = D_\gamma \cup D_{\overline{\gamma}} \cup D_{\gamma_u}$$

where D_γ, $D_{\overline{\gamma}}$ and D_{γ_u} correspond to the stability domains where performance is guaranteed, non-performance is guaranteed and performance is undetermined respectively, with probabilities $p\left(D_\gamma\right)$, $p\left(D_{\overline{\gamma}}\right)$ and $p\left(D_{\gamma_u}\right)$. Guaranteed bounds on the exact probability $\overline{P}^{\gamma}_{\mathbf{\Delta},f}\left(M(s)\right)$ of non-performance follow, thus solving Problem 2:

$$p\left(D_{\overline{\gamma}}\right) \leq \overline{P}^{\gamma}_{\mathbf{\Delta},f}\left(M(s)\right) \leq p(D_s) - p\left(D_\gamma\right) = p\left(D_{\overline{\gamma}}\right) + p\left(D_{\gamma_u}\right)$$

The only difference with stability is that the investigated domain is limited to the domain of guaranteed stability D_s, since performance analysis only makes sense for stable systems. The following partition of the normalized uncertainty domain $\mathcal{B}_\delta$ is finally obtained:

$$\mathcal{B}_\delta = D_\gamma \cup D_{\overline{\gamma}} \cup D_{\gamma_u} \cup D_{\overline{s}} \cup D_{s_u}$$

In other words, the uncertain system does not meet the performance requirement for a given uncertainty $\Delta \in \mathbf{\Delta}$ if it is unstable or the H_∞ norm exceeds the desired threshold γ.

Finally, stability margin analysis follows the same scheme. The considered margin is first computed at the center of $\mathcal{B}_\delta$, *i.e.* for the nominal system $\Delta = 0$. If it is larger (resp. smaller) than the desired threshold ϕ, it is then checked whether the margin requirement is satisfied (resp. violated) on the entire domain $\mathcal{B}_\delta$, using sufficient conditions involving μ upper bound computations (see Propositions 3.1 and 3.3 of [10] for gain/phase/disk margins, and Propositions 4.1 and 4.3 of [11] for delay margin). If this cannot be guaranteed, $\mathcal{B}_\delta$ is finally partitioned into smaller boxes and this process is repeated until each box has guaranteed sufficient/insufficient margin, or is small enough to

be neglected. Guaranteed upper and lower bounds on the exact probability of margin violation $\overline{P}_{\Delta,f}^{\phi}\left(M(s)\right)$ are finally obtained, based on the probability distributions of the uncertain parameters, thus solving Problem 3.

3 MICROSATELLITE CASE DESCRIPTION

3.1 Description of the satellite test case

Microcarb is a mission aiming at monitoring the CO_2 surface fluxes on Earth in order to improve our knowledge on the mechanisms governing the exchanges between the sources and the sinks, and their evolution [15]. The concentration measurement will be performed by a passive Short Wave Infrared spectrometer that will measure the solar light reflected by the Earth surface in the near infrared. By deducing the depth of the absorption lines in the measured spectra, the CO_2 concentration can be deduced.

The AOCS system has been developed, tested and validated by CNES. The development phase including the AOCS validation is finished and has been carried out using the classical process of AOCS control loop validation at CNES.

Microcarb AOCS is inherited from the generic Myriade platforms composed of four modes described in [17] and shown in Figure 2.

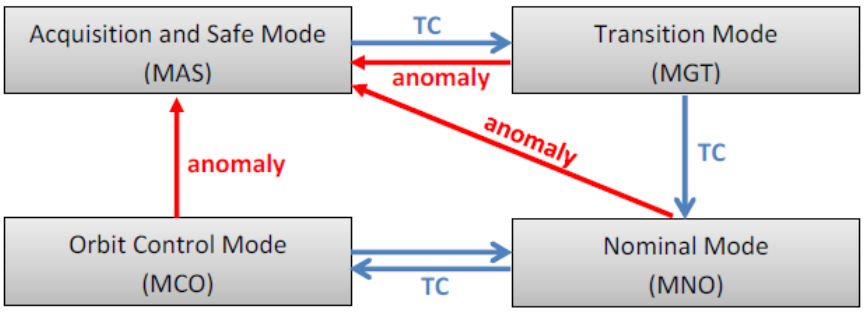

Figure 2. Myriade AOCS modes

The MAS is the AOCS mode reached after launcher separation, and is used in case of anomaly on the satellite. The MGT is a transition mode from MAS to the MNO where the mission can take place nominally. The MNO is a 3-axes control mode based on star tracker measurements for the attitude estimation and on four reaction wheels for the attitude control. The wheel unloading is provided by three magnetorquer bars.

The MCO is used for orbit control manoeuvers. The actuation is performed by four thrusters commanded in off-modulation and a gyroless MCO has been implemented thanks to a star tracker. It should be noted that this mode is historically based on gyrometer measurements for Myriade platforms [16]. However, the design of this mode has been updated thanks to a new star tracker that is able to withstand the dynamics of the spacecraft during this mode of operation and is robust to the Moon in its field of view [16]. Modifications of the control loop have therefore been performed for Microcarb as well as specific validation on this AOCS mode.

During typical operational phases, the satellite will be in MNO and in MCO. The mission requires a challenging agility due to various pointing modes described in [16]. The specifications in terms of absolute pointing error and agility are given in [16]. In order to meet the specifications, the AOCS algorithms have been upgraded in MNO with respect to the historical Myriade platform and are also detailed in [16].

3.2 Description of the attitude control law of the normal mode

The structure of the controller does not show differences with respect to the other Myriade satellites. When the pointing error is high, the control is performed by a velocity bias controller whose duty consists in refining the pointing performance without saturating the reaction wheels.

Under a certain threshold of pointing error, the control is switched to a Proportional Derivative controller. An integrator to reject the external perturbations and a filter to reject the flexible modes while compensating the delay effects are added to obtain the following controller structure [16]:

$$\boldsymbol{K(s) = \left(K_p + K_d s\right) \frac{1}{s} \frac{1}{1+\tau_1 s} \frac{1+\tau_2 s}{1+\tau_3 s}} \quad (2)$$

Microcarb satellite includes a rotating solar panel that presents flexible modes. This rotation creates a varying projection of these flexible modes on the satellite main axes depending on the current rotation angle of the solar panel. This solar panel is however designed so that the frequencies of the flexible modes are higher than the bandwidth of the AOCS control loop, enabling a gain rejection strategy. The unloading controller, which has a very small bandwidth compared to the reaction wheel loop, is not considered here and does not impact the robust stability of the system.

Suitable numerical values for the gains of the controller (2) have been optimized with the structured H_∞ design method presented in [18] according to the requirements expressed in [16] and recalled below. These constraints apply to the transfer function between the target and measured attitudes (θ/θ_{target}):

- The bandwidth of the closed-loop system must be lower than the bandwidth of the inner wheel controller to avoid interaction between the two control laws,
- The bandwidth of the closed-loop system must be larger than the highest guidance profile frequency,
- The phase margin must be larger than 20 degrees and the gain margin must be larger than 6 dB.

Constraints also need to be defined on the transfer function between the disturbing torques and the measured attitude (θ/T_{dist}):

- The gain of this function must be lower than -36 dB for frequencies larger than 1Hz to ensure flexible modes rejection,
- The gain of this function transfer must be lower than 10.85 dB on the bandwidth of the closed-loop transfer θ/θ_{target}, to ensure that the error induced by a 0.1 Nm torque is lower than 0.02 degrees for this frequency domain.

In order to reduce the pointing error more rapidly by improving the reactivity of the control system, a feed-forward contribution has been added to the control law [16] but is not detailed here since it does not affect the stability analysis.

3.3 Description of the attitude control law of the orbit control mode

The MCO controller is also based on a Proportional Derivative controller and a roll-off filter which is tuned to reject the flexible modes and improve the performance. Because of the large uncertainties on the thruster dynamics, a high conservativeness in terms of stability margins is required, inconsistent with the inclusion of a pure integrator in the control law. The rejection of constant disturbance torques is nevertheless necessary, especially because misalignment of the thrusters and uncertainties on the knowledge of the centre of mass of the satellite may induce a significant constant part on the disturbance torque. In addition, the rotation of the solar panel modifies the position of the centre of mass, thus changing the value of the disturbance torque from one thrust to another, making it hard to find an a priori correct value. Therefore, an estimator of the disturbance torques is added in the design. The control loop also contains an allocation module that distributes the commands among the thrusters. Note that neither the control allocator nor the estimator have been considered in our robustness analysis strategy which only focused on the proportional derivative controller and the filter. The latter were designed using classical control theory tools.

4 APPLICATION OF PROBABILISTIC μ-ANALYSIS TO THE MICROCARB CASE

The study case we focus on in this paper is the validation phase of the Microcarb control laws in the normal mode of operation (MNO) and in the orbit control mode (MCO). In the process of designing the controllers and validating them, simplified linear models are developed. In particular, Linear Fractional Representations (LFR) are required for the Matlab H_∞ design tool. Since parametric variations are not included in the H_∞ design (but may be included in the gain and phase margin requirements), the models are not in a minimal form. After several iterations between the controller design and the requirements, a suitable controller is obtained.

Validation of this controller with respect to the defined specifications and parametric variations is then carried out. Performance and robustness of the nominal case (with nominal parameter values) are first evaluated. Then, a robust stability analysis consisting in finding the worst cases with respect to the possible parametric variations is performed. Time-domain simulations are finally carried out to check the performance, and a set of specific studies on points identified as requiring attention are also carried out before launching the pseudo-Monte-Carlo campaigns. For a description of these campaigns, one can refer to explanations in [16].

In the present study, the goal is rather to assess the μ-analysis and probabilistic μ-analysis toolboxes provided by ONERA and developed in the frame of a joint research program (see Section 2). To do so, the idea is to respect the validation process carried out in the CNES Microcarb project and integrate these tools as a preliminary means of robust stability and performance analysis, just after the design of the controllers. In particular, evaluating the worst-case combination of uncertainties can be tedious if a large number of uncertainties are present, and may lead to mistakes if the worst combination of parameters expected does not correspond to boundary values of the parameters. However, μ-analysis does not provide time performance information, so we limit the comparison of the classical validation approach at CNES with the use of the SMART [21] and STOWAT [9] toolboxes developed at ONERA to robust stability and frequency analyses.

4.1 Validation of the normal mode

4.1.1 System modelling

For the MNO case, let us first define the simplified model of the control loop used for the analysis. The dynamics of the satellite is assumed as a rigid body, with decoupled dynamics along each principal inertia axis. The introduction of flexible modes is however necessary for validation since it impacts the robustness of the system. In this analysis, only the first flexible mode is considered. The considered uncertain parameters of the system dynamics are therefore:

- The diagonal terms of the inertia matrix,
- The eigenfrequency of the flexible mode,
- The damping ratio of the flexible mode.

The rotation modal participation factor in the satellite reference frame is assumed known and not varying (worst-case considered).

Since the controller design is conservative with respect to the impact of the flexible modes, it is assumed in this analysis that the rotational and the translational movements of the solar panels are decoupled. A first order Padé approximation is included in the control loop to account for the delays. In addition to the controller, a speed reconstruction filter and a dynamics modelling of the actuators are present in the control loop without including uncertain parameters.

This quite simple model however represents the main characteristics of the normal mode. On each satellite axis, the classical minimal LFT representation of a flexible mode has been implemented, and three uncertain parameters with associated truncated normal distributions have been considered.

It should be noted that models of increasing complexity have been implemented and analysed with the μ-analysis based toolboxes SMART and STOWAT. However, here are some advices for AOCS engineers:

- Probabilistic μ-analysis should not be used for systems with only one parametric uncertainty, other classical control methods such as the root locus are better suited,
- When possible, to reduce complexity, uncertain parameters which have a negligible impact on stability should be removed. This step can be achieved by a sensitivity analysis.

Therefore, it is better to consider directly all the most relevant uncertain parameters in the probabilistic μ-analysis.

4.1.2 Stability and robustness of the nominal system

First, the stability and the robustness of the nominal system have been evaluated. The resulting gain, phase and delay margins are reported in Table 1.

Table 1. Margins of the nominal system

	Gain margin [dB]	**Phase margin [deg]**	**Delay margin [s]**
X_S axis	-6.1, 6.3	23.1	>1

The results obtained are perfectly compliant with the margins reported during the validation process, which proves the quality of the model implemented.

4.1.3 Worst case analysis

The results presented in this subsection refer to the X_s axis of the satellite reference frame.

Table 2. Worst-case gain margin

Lower bound	-4.24 dB
Upper bound	-4.52 dB

Table 3. Worst-case phase margin

Lower bound	20.3 deg
Upper bound	21.3 deg

Tables 2 and 3 report respectively the worst gain and phase margins obtained with the function iomargins of the SMART Library of the SMAC Toolbox [21]. In order to make the algorithm converge in 100 iterations, it is necessary to shrink the frequency interval in which the search for the worst-case condition is conducted. Knowing that the most critical gain margin on the X_s axis reported in Table 1 is found at a frequency of near 0.1 rad/s, the μ-analysis was finally performed on a range spanning between 0.1 rad/s and 1 rad/s. The same frequency interval can be reasonably adopted also for the worst-case phase margin analysis, as the nominal value of 23.1 deg reported in Table 1 for X_s is found near 0.2 rad/s.

Here again, the results are fully compliant with those obtained during the validation process.

4.1.4 Probabilistic worst case analysis

At this point, the probabilistic μ-analysis is performed by calling the function mupb of the STOWAT toolbox. The algorithm stops dividing the uncertainties domain when the probability of the single box is below 0.001%. The results are reported in Figure 3.

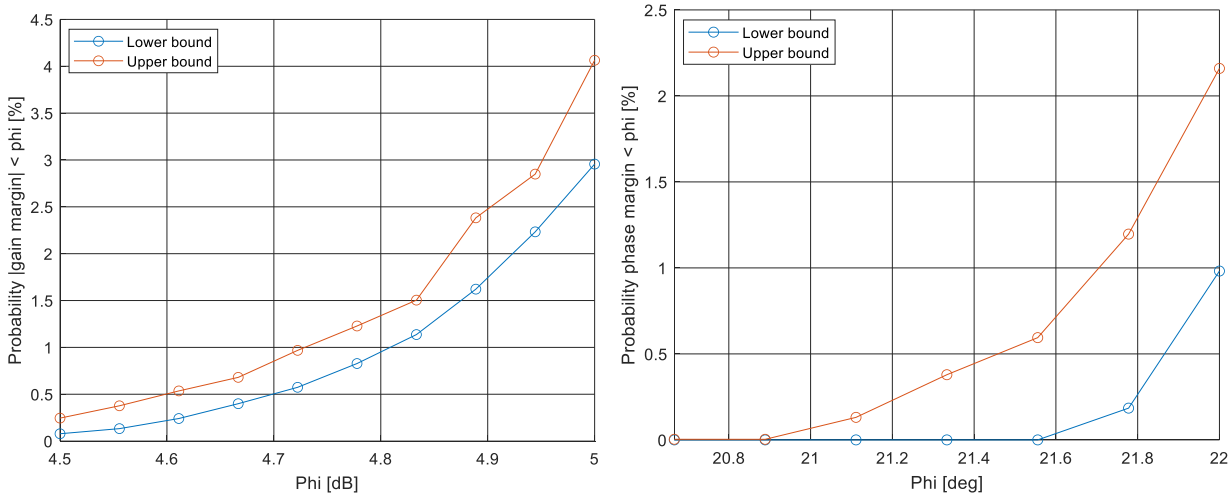

Figure 3. Probability that |gain margin| < phi: uniform distribution (left), truncated normal distribution (right)

The probability that the margins remain below a certain threshold phi increases monotonically with the value of phi. Similar results are obtained with the phase margin.

4.1.5 Conclusion for the MNO case

For this mode, compared to the robust analysis performed by the project, a minimal representation of the system has been developed. However, given the simplicity of the dynamics transfer function, this minimal LFR has been easily achieved. For this case, the robust analysis gives similar results as the validation study of the project which gives confidence in the precision of the method. Since there is

only one main uncertain parameter (the inertia value) that has a major impact on the robustness, the robustness analysis is rather simple but shows that the μ-analysis can be used even if in simple cases the gain in time is limited. The probabilistic μ-analysis gives more information on the distribution of probability that can be useful for the project.

4.2 Validation of the orbit control mode

4.2.1 System modelling

In this case, the robustness of the system with respect to the flexible modes is more critical because there is a risk of coupling between the thrusters and the solar panel dynamics. Therefore, for the validation analysis, two models of the dynamics of the system are used:

- A simplified model similar to the one used in Section 4.1.1.
- A complete model developed at CNES, which takes into account the coupling effects between the satellite axes as well as the relative rotation between different parts of the structure (similar to the model developed in [20]). The true dynamics equations are implemented, including the rotation and translation modal participation of the flexible modes.

As for the MNO, only one flexible mode is considered in the analysis since the robustness for the other modes is very high. The angle of the solar panel also varies and modifies the impact of the flexible modes on the system.

For the design and validation analysis of the controllers, the complete model linearized at the worst-case value of solar panel angle is used. However, this model cannot be easily put in a minimal form given the formulation of the equations, contrary to the simplified model. Tools like those used in [19] and [20] could help achieving minimal or nearly minimal representations.

For the controllers, at this stage of the process, two controllers remained possible:

- One with the same stabilizing filter used for the Taranis mission, more conservative,
- One with the stabilizing filter tuned for Microcarb with a higher bandwidth.

Both were studied and considered. The Padé approximation for the delay is kept and the delay value is this time considered an uncertain parameter as critical in the robustness of this mode.

The uncertain parameters are therefore:

- The inertia matrix, with a constant uncertainty applying on all the terms simultaneously,
- The eigenfrequency of the flexible mode, with a truncated normal distribution,
- The damping ratio of the flexible mode, with a truncated normal distribution,
- Time delay with a uniform distribution between the minimal and maximal values.

Four parameters are uncertain and considered in the analysis.

The following results refer specifically to the X_S axis of the satellite reference frame, but analogous considerations can be obtained for the other cases. For the sake of brevity, only the results with the complex model are presented. The validation of the simplified model has shown, like for the MNO, identical results with the process carried out in the CNES project. Also, only the results with the controller designed specifically for Microcarb are presented.

4.2.2 Stability and robustness of the nominal system

The stability of the system is first evaluated in the nominal conditions. The results in terms of gain, phase and delay margins are collected in Table 4.

Table 4. Margins of the nominal system

	Gain margin [dB]	Phase margin [deg]	Delay margin [s]
X_S axis	14.6, 67.0	56.1	>3s

As expected, the margins of Table 4 coincide with the values reported in the project at this stage.

4.2.3 Worst case analysis

Tables 5 and 6 report respectively the worst gain and phase margins obtained with the function iomargins contained in the SMART Library of the SMAC Toolbox. In order to obtain reasonable results, it is necessary to shrink the range of frequencies in which the worst-case search is realized. As the most stringent nominal gain of Table 4 is found at a frequency near 1.1 rad/s, the μ-analysis is performed in a range between 0.1 rad/s and 10 rad/s. The interval used for the worst-case phase analysis, instead, spans between 0.2 and 0.5 rad/s, range which includes the frequency of the nominal phase margin.

Table 5. Worst-case gain margin

Lower bound	13.1 dB
Upper bound	13.4 dB

Table 6. Worst-case phase margin

Lower bound	53.0 deg
Upper bound	55.6 deg

The upper margins identified in Tables 5 and 6 exactly coincide with the values determined for the MCO. This result is particularly significant as it proves that the iomargins routine is capable of properly determining the worst-case robustness of the system. Furthermore, the algorithm is extremely fast as it produces the results of Tables 5 and 6 in 17.3 s and 1.8 s respectively. The validation procedure classically used, on the contrary, consists in evaluating the robustness of the systems for different combinations of the uncertain parameters. Iomargins can thus drastically shorten the time-consuming validation process usually adopted in space projects, allowing better compliance with the stringent requirements of rapidity in the design of space missions. It is interesting to notice that the worst combination of the uncertainty parameters found by iomargins slightly differs with the prevision of the project which sets the worst eigenfrequency and the worst damping at the lower bound of the uncertainty domain. This fact, however, is not relevant from the point of view of the margins themselves, which do not significantly depend on either the eigenfrequency or the damping of the flexible mode.

4.2.4 Probabilistic worst case analysis

At this point, the same problem has been tackled from a probabilistic perspective by calling the function mupb of the STOWAT. The algorithm stops dividing the uncertainties domain when the probability of the single box gets below 0.001%. The cutting procedure is optimized by making use of the μ sensitivities. The range of frequencies over which the search for the μ value is performed is set between 0.1 rad/s and 10 rad/s for the case of the gain margin and between 0.01 rad/s and 1 rad/s for the case of the phase margin. Figure 4 reports the probability that the gain margins of the system remain below a certain threshold.

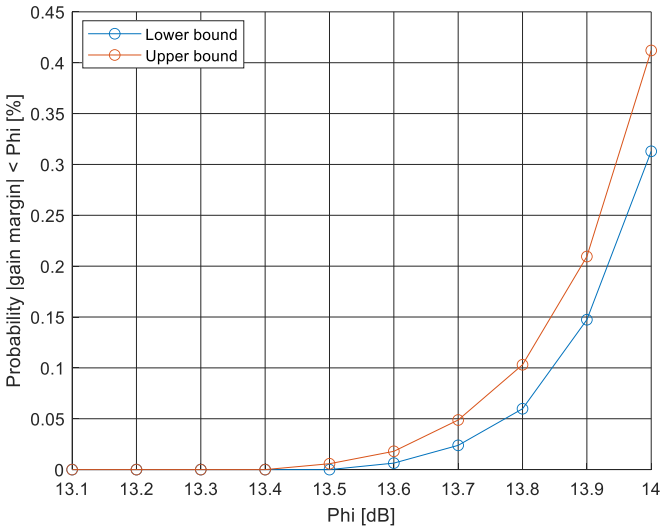

Figure 4. Probability that the gain margin remains below a certain threshold

4.2.5 Conclusion for the MCO case

In this case, the criticality of the flexible mode interaction with the control required a more complex modelling and worst case analysis. The μ-analysis and the probabilistic μ-analysis showed a great advantage, making worst case analysis simpler, faster and more reliable with the guarantee that worst combinations are correctly found. Moreover, the probabilistic μ-analysis, by showing the evolution of the probability that gain or phase margins get lower than a given threshold, gives access to some additional information which can be helpful for instance to choose between two possible controllers. The drawback of the method is however that it remains sensitive to the minimality of the representation. Some expertise is then still needed at the modelling level to use the tools in the more favourable conditions.

5 CONCLUSION

In this paper, recent advances in probabilistic μ-analysis have been presented and tested on a real satellite project carried out. The goal was to identify where these tools could be helpful in the V&V process by first replacing some analyses usually performed with slower procedures in a real space project and save time while providing relevant information on the designed controller. The robustness analysis performed right after the design phase is crucial to validate the control loop before launching the Monte-Carlo simulation campaigns, for detecting potential issues that could be whether accepted if the probability of occurrence is low or leading to a new controller design. At this stage (before Monte-Carlo simulation campaigns), iterating on the controller is indeed not very costly.

These tools have been tested for replacement of classical worst-case analysis in the Microcarb test case. This satellite has the advantage of having challenging pointing and agility constraints. While for the MNO, the complexity of the model is low and thus does not result in a specific gain in terms of time saved in the process of validation; for the MCO, the higher complexity and number of uncertainties on the model needed especially for the robustness with respect to the flexible modes showed a direct realized gain. The tedious worst-case research (performed with actual process) with both filters gave the same results as those obtained much more rapidly with the advanced μ-analysis tools. Moreover, the latter provide some guarantees. The drawback is however that a minimal LFT representation is needed to avoid numerical issues. While it is straightforward to obtain a minimal

model for a single-axis satellite with one flexible mode, more representative models with projections of flexible modes on different axes are difficult to obtain in a minimal form. Specific modelling tools or procedures at least to get closer to minimality could be helpful to go towards an industrialization of the toolbox, for instance [19].

Future work will consist in continuing the improvement of the STOWAT toolbox and the reflexion on the modification of the V&V process. Indeed, this study was focused on integrating the tool without modification of the V&V process to show its ease-of-use, precision and engineer time-saving potential characteristics, as well as limitations for future research studies; but its interest may be to enable an evolution of the validation process in the frame of faster AOCS development and validation with more targeted Monte-Carlo campaigns. The reflection, development and testing continue in order to make the most of the new tools provided by the research community.

6 REFERENCES

[1] K. Zhou, J. Doyle, K. Glover, *Robust and optimal control*, Prentice-Hall, 1996.

[2] G. Ferreres, *A practical approach to robustness analysis with aeronautical applications,* Kluwer Academic, 1999.

[3] S. Khatri, P. Parrilo, "Guaranteed bounds for probabilistic μ", In: *Proceedings of the IEEE Conference on Decision and Control*, pp. 3349–3354, 1998.

[4] G. Balas, P. Seiler, A. Packard, "Analysis of an UAV flight control system using probabilistic μ", *In: Proceedings of the AIAA Guidance, Navigation, and Control Conference*, 2012.

[5] A. Marcos, S. Bennani, C. Roux, "Stochastic μ-analysis for launcher thrust vector control systems", *In: Proceedings of the CEAS EuroGNC Conference*, 2015.

[6] A. Falcoz, D. Alazard, C. Pittet, "Probabilistic μ-analysis for system performances assessment". *In: Proceedings of the IFAC World Congress*, IFAC-PapersOnLine 50(1), pp. 399–404, 2017.

[7] S. Thai, C. Roos, J.-M. Biannic, "Probabilistic μ-analysis for stability and H_∞ performance verification", *In: Proceedings of the American Control Conference*, pp. 3099–3104, 2019.

[8] J.-M. Biannic, C. Roos, S. Bennani, F. Boquet, V. Preda, B. Girouart, "Advanced probabilistic μ-analysis techniques for AOCS validation", *European Journal of Control*, 62, pp. 120–129, 2021.

[9] C. Roos, J.-M. Biannic, H. Evain, "A new step towards the integration of probabilistic μ in the aerospace V&V process", *CEAS Space Journal*, 2023.

[10] F. Somers, S. Thai, C.Roos, J.-M. Biannic, S. Bennani, V. Preda, F. Sanfedino, "Probabilistic gain, phase and disk margins with application to AOCS validation", *In: Proceedings of the IFAC Symposium on Robust Control Design*, IFAC-PapersOnLine 55(25), pp. 1–6, 2022.

[11] F. Somers, C. Roos, F. Sanfedino, S. Bennani, V. Preda, "A μ-analysis based approach to probabilistic delay margin analysis of uncertain linear systems". *In: Proceedings of the IEEE Conference on Control Technology and Applications*, 2023.

[12] C. Roos, F. Lescher, J-M. Biannic, C. Döll, G. Ferreres, “A set of μ-analysis based tools to evaluate the robustness properties of high-dimensional uncertain systems”, *In: Proceedings of the IEEE Multiconference on Systems and Control*, pp. 644–649, 2011.

[13] C. Roos, J-M. Biannic, “A detailed comparative analysis of all practical algorithms to compute lower bounds on the structured singular value”, *Control Engineering Practice*, *44*, pp. 219–230, 2015.

[14] A. Packard, J. Doyle, “The complex structured singular value”, *Automatica*, 29(1), pp. 71–109, 1993.

[15] V. Pascal, C. Buil, E. Cansot, J. Loesel, L. Tauziede, C. Pierangelo, F. Bermudo, “A new space instrumental concept based on dispersive components for the measurement of CO2 concentration in the atmosphere”, *In: Proceedings of the International Conference on Space Optics*, 2012.

[16] G. Rineau, S. Delavault, F. Genin, “Microsatellite AOCS design for the agile mission Microcarb”, *In: Proceedings of the International ESA Conference on Guidance, Navigation & Control Systems*, 2021.

[17] M. Le Du, J. Maureau, P. Prieur, “Myriade: an adaptative AOCS concept”, *In: Proceedings of the International ESA Conference on Guidance, Navigation & Control Systems*, 2002.

[18] C. Pittet, F. Viaud, J. Mignot, “Attitude and active payload control: the H_∞ revolution”, *In: Proceedings of the IFAC World Congress*, IFAC-PapersOnLine 50(1), pp. 6440–6445, 2017.

[19] D. Alazard, F. Sanfedino, “Satellite dynamics toolbox for preliminary design phase”. In: *Proceedings of the 43rd Annual AAS Guidance and Control Conference*, pp. 1461-1472, 2020.

[20] C. Cumer, D. Alazard, A. Grynagier, C. Pittet-Mechin: “Codesign mechanics / attitude control for a simplified AOCS preliminary synthesis”. *In Proceedings of the International ESA Conference on Guidance, Navigation & Control Systems*, 2014.

[21] C. Roos: “Systems Modeling, Analysis and Control (SMAC) toolbox: an insight into the robustness analysis library”. *In: Proceedings of the IEEE International Symposium on Computer-Aided Control System Design*, pp. 176–181, 2013. Available with the SMAC Toolbox at w3.onera.fr/smac/smart.